Military Technical College
Kobry El-Kobbah,
Cairo, Egypt.

18th International Conference on Applied Mechanics and Mechanical Engineering.

INVESTIGATION OF THE OPERATION OF AN ELECTRO-HYDRAULIC CONTROL SYSTEM OF A FLYING VEHICLE UNDER FAILURE CONDITIONS

M. Z. Fadel[1,*], M. G. Rabie[2] and A. M. Youssef[1]

ABSTRACT

Electro-hydraulic system technology is employed in many modern control systems including aircrafts and missile flight control systems. These systems used to position the control surfaces of the flying vehicles with high controllability and accurate action. Pilot or autopilot commands are translated into electrical position commands to the electro-hydraulic control system (EHCS). This study is based upon the development of a detailed nonlinear mathematical model of the EHCS and a computer simulation program using MATLAB/SIMULINK package. The EHCS mainly consists of two systems; main and secondary with two separate active hydraulic power supply systems, used to supply the EHCS with the required power. The studied EHCS incorporates two electro-hydraulic servo-valves and a smart design of built-in direct operated directional control valves, controlled by electrical solenoids. The EHCS is designed with smart capability to over-ride the possible problems of failure in the hydraulic power supply systems or in the servo-valves. The transient response is obtained by the simulation program using the solver of ode23s (stiff/Mod. Rosenbrock) method. A comparison between the dynamic responses of the EHCS is presented in different modes of failure. The simulation results show that this EHCS is capable to provide a continued safe flight even when experiencing a certain component failure or a combination of failures.

KEYWORDS

Electro-Hydraulic Control System (EHCS), Servo-Valve, Electrical Solenoid, Directional Control Valve, Modes of Failure, Dynamic Response.

---

[1] Egyptian Armed Forces.
[2] Professor, Nodern Academy for Engineering and Technology, Cairo, Egypt.

INTRODUCTION

The use electro-hydraulic systems are becoming more wide spread in industry accompanied by a growing interest in digital control. These systems are the core component of servo control systems. This class of control systems is traditionally called by Fly-By-Wire systems (FBW). The use of the FBW systems for flight control of aeronautical vehicles has increased steadily in the recent years. The FBW is a system that replaces the conventional manual flight controls of an aircraft with an electronic interface. The movements of flight controls are converted to electronic signals transmitted by wires, and flight control computers determine how to move the actuators at each control surface to provide the ordered response. The marriage between electronics and hydraulic power systems has led to many powerful and precise control systems, saving much energy and money [1].

This concept is applied in the electro-hydraulic control systems (EHCS). These systems have the same advantages as hydraulic power systems, particularly the maximum power to- weight ratio and the high stiffness of hydraulic actuators. They also have the same advantages as electronic controllers, particularly in regard to high controllability and precision. Due to its advantages, these systems have been applied in many fields, such as astronavigation, aviation, navigation, and military equipment [2]. These systems may be called electro-hydraulic servo systems.

The electro-hydraulic servo system refers to the control system which combined two control modes of electrical and hydraulic. Detecting, transmitting and processing the signal by use of electric and electronic components, driving the load with hydraulic transmission in the electro-hydraulic servo control system. So it can make full use of electrical system for its convenience and aptitude, make full use of hydraulic system for its rapid response speed, big load stiffness and accurate positioning characteristics to make the whole system more adaptable [3].

The studied EHCS incorporates two electro-hydraulic servo-valves (EHSV) and a smart design of four built-in direct operated directional control valves (DCV) controlled by four electrical solenoids and a switching DCV works as ON-OFF switch of the EHSV as shown in (fig. 1). The detailed non-linear mathematical model is deduced to each component of the EHCS. The MATLAB/ SIMULINK package is used to develop a simulation program to obtain the transient response of the EHCS. Simulink is a graphical environment for dynamic system modeling, simulation and analysis interactively. A complex system simulation model is built using Simulink environment to simplify the model, using M files to determine the system initial parameters[4]. The simulation programs are built considering numerical values of a typical electrohydraulic servo system incorporating a two-stage servo valve[5].

The essential inputs to the main and secondary systems of this EHCS are the pressure supply and electrical current signal to the EHSV which is one of the most failure prone components, and has a direct and significant impact on the performance and reliability of the entire servo control system [6]. Thus, it is very important to analyze the failure modes of the EHSV and the pressure source and their effect on the EHCS operation by obtaining the transient response of our studied EHCS in case of each mode of failures and compare it to the original response of the system [7].

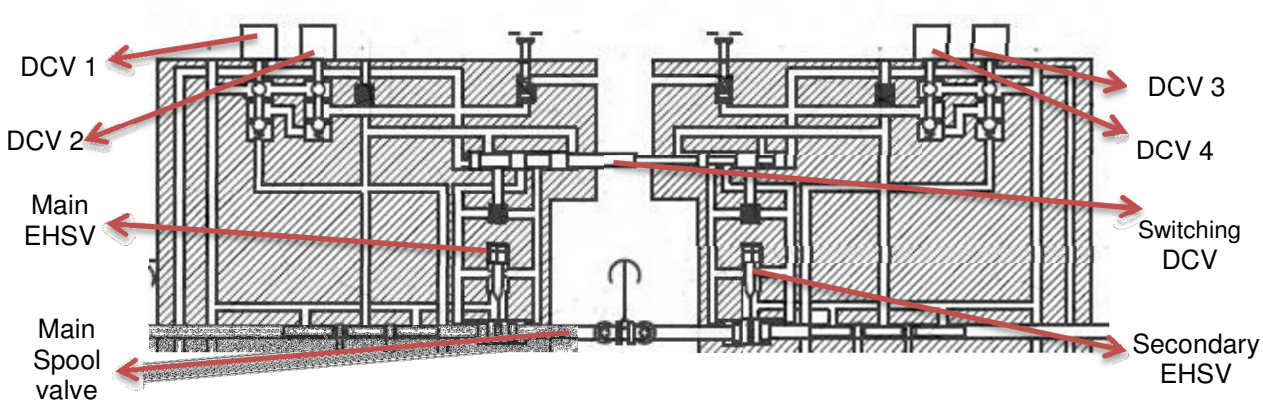

Fig. 1. ISA Scheme.

WORKING PRINCIPLE THE STUDIED EHCS

When the main power system is operating reliably and its solenoids energized, a control signal reaches successfully the both main and secondary electric solenoids and EHSV's. As the control signal reaches the two electric solenoids, the direct operated DCV is opened allowing the high pressure to push the switching DCV to the right (due to the pressure subjected to the greater area of the switching DCV). This motion of the switching DCV causes the high pressure connecting with the main EHSV and by-passing the secondary EHSV. The flapper valve in the EHSV produces a very small pressure difference, just sufficient to equilibrate the feedback spring force. The deflection of the flapper to the right causing the main spool driving piston moved to the left [8], [5].

Due to the complicated system, the dynamic behavior of this EHCS is described by the following set of mathematical relations. The pressure losses of the transmission lines are neglected and the pressure supply in the system is considered to be constant.

MATHEMATICAL MODEL OF THE EHCS

Poppet Type DCV

The EHCS incorporates four 3/2 DCV of spherical poppet type. These four DCV's are direct operated, controlled by electric solenoids. Figure 2 shows the first valve. In this position, the poppet 2 is seated, closing the line (P). Meanwhile, the poppet (4) is unseated connecting the ports (A) and (T).

The valve operation with energizing the solenoid (S1) is shown by Fig. 3. During this operating mode, the poppet (4) is seated to disconnect ports (A) and (T). In the same time, poppet (2) is unseated to connect ports (A) and (P).

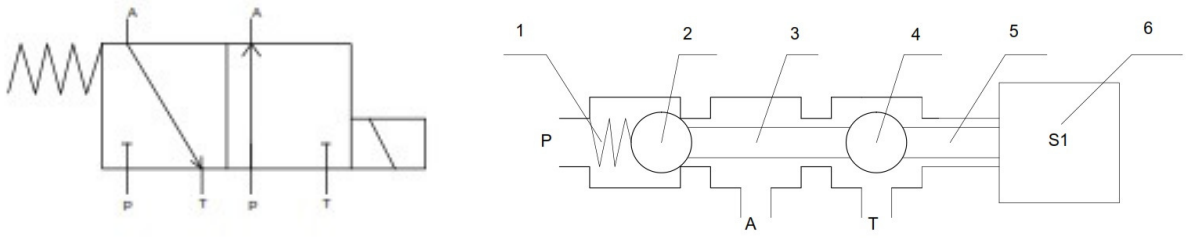

1.Spring, 2.Left poppet, 3.Rod, 4.Right poppet, 5.Core, 6.Solenoid

Fig. 2. 3/2 poppet DCV (out of operation).

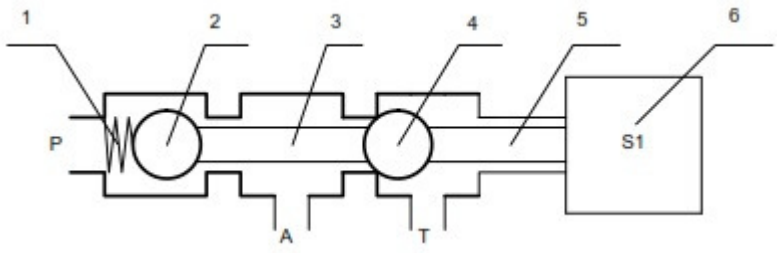

Fig. 3. 3/2 poppet DCV (in case of operation).

First Direct Operated DCV Model

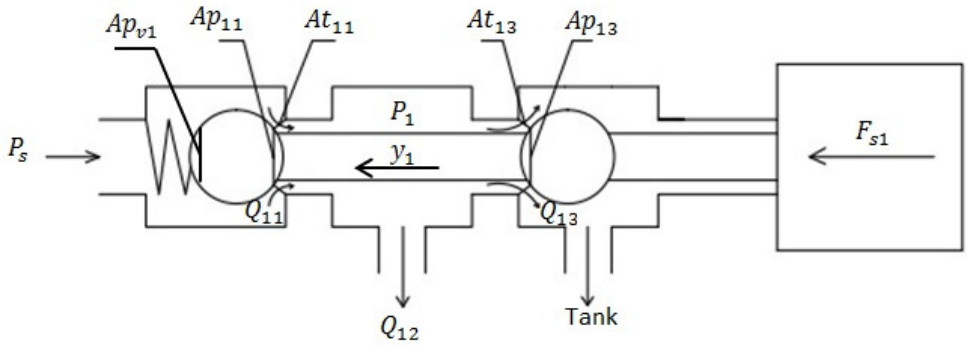

Fig. 4. First DCV operation**.**

Equation of motion

By energizing the electric solenoid (S1), the solenoid force ($\mathrm{F_{s1}}$) acts on the moving parts against the pressure forces, spring forces, seat reaction forces, viscous friction forces and inertia forces, Fig. 4. The motion during this mode is described by the following relations:

$$\mathrm{F_{S1}} = \mathrm{m\ddot{y}_1} + \mathrm{f_v\dot{y}_1} + \mathrm{K_{sp}(y_o + y_1)} + \mathrm{P_{S1}Ap_{v1}} - \mathrm{P_1Ap_{11}} + \mathrm{P_1Ap_{13}} - \mathrm{F_{SR1}} \qquad (1)$$

where

$\mathrm{Ap_{v1}}$ Subjected area to the pressure on the left poppet, $\mathrm{m^2}$

$\mathrm{Ap_{11}}$ Resultant subjected area to the pressure on the left poppet, $\mathrm{m^2}$

Ap_{13} Resultant subjected area to the pressure on the right poppet, m^2
F_{S1} Solenoid force of the first DCV, 200 N
F_{SR1} Total seat reaction force of the first DCV, N
K_{sp} Spring stiffness,15000 N/m
P_1 Pressure in the first valve chamber, Pa
P_{S1} Supply pressure of the main system of EHCS, 300 bar
f_v Spring damping coefficient, 300 Ns/m
y_1 First DCV displacement, m
y_o Spring pre-compression distance, 3 mm
m Reduced mass of the moving parts of first DCV, 0.01 Kg

Seat reaction force

The poppet displacement in the closure direction is limited mechanically. When reaching its seat, a seat reaction force takes place due to the action of the structural damping of the seat material.

$$F_{SR1} = F_{1L} - F_{1R} \tag{2}$$

$$F_{1L} = \begin{cases} 0 & y_1 > 0 \\ -K_{sm}y_1 - f_{sm}\dot{y}_1 & y_1 \le 0 \end{cases} \tag{3}$$

$$F_{1R} = \begin{cases} 0 & y_1 < y_i \\ K_{sm}(y_1 - y_i) + f_{sm}\dot{y}_1 & y_1 \ge y_i \end{cases} \tag{4}$$

where

F_{1L} Seat reaction force for the left poppet, N
F_{1R} Seat reaction force for the right poppet, N
K_{sm} Seat material stiffness, $1 * 10^7$ N/m
f_{sm} Seat material structural damping coefficient, 5000 Ns/m
y_i The initial distance between the right poppet and its seat, 2 mm

Flow rates through the throttling areas

There are two flow rates through the two throttling areas At_{11} and At_{13} . These flow rates are given by the following expressions:

$$Q_{11} = C_d At_{11}\sqrt{\frac{2(P_{S1} - P_1)}{\rho}} \tag{5}$$

$$Q_{13} = C_d At_{13}\sqrt{\frac{2(P_1 - P_t)}{\rho}} \tag{6}$$

where

Q_{11} Throttle flow rate of the left poppet, m^3/s
Q_{13} Throttle flow rate of the right poppet, m^3/s
At_{11} Throttle area of the left poppet, m^2
At_{13} Throttle area of the right poppet, m^2

C_d	Discharge coefficient, 0.611
ρ	Oil density, 900 Kg/m^3
P_t	Return tank pressure, 2 bar

Combined Direct Operated DCV Model

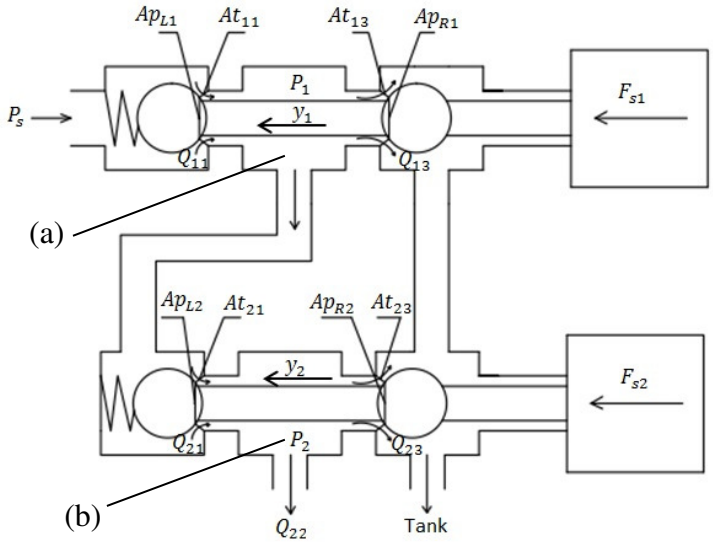

Fig. 5. Scheme of the combined direct operated DCV**.**

Equation of motion

The motion of this combined DCV (shown in fig. 5) is described by the following relation:

$$F_{S2} = m\ddot{y}_2 + f_v\dot{y}_2 + K_{sp}(y_o + y_2) + P_1Ap_{v2} - P_2Ap_{21} + P_2Ap_{23} - F_{SR2} \quad (7)$$

where

F_{S2}	Solenoid force of the second DCV, 200 N
F_{SR2}	Total seat reaction force of the Second DCV, N
P_2	Pressure in chamber (b), Pa
Ap_{21}	Resultant subjected area to the pressure on the left poppet, m^2
Ap_{23}	Resultant subjected area to the pressure on the right poppet, m^2
y_2	Second DCV displacement, m
Ap_{v2}	Subjected area to the pressure on the left poppet, m^2

Seat reaction force

The poppet displacement in the closure direction is limited mechanically. When reaching its seat, a seat reaction force takes place due to the action of the structural damping of the seat material.

$$F_{SR2} = F_{2L} - F_{2R} \quad (8)$$

$$F_{2L} = \begin{cases} 0 & y_2 > 0 \\ -f_{sm}\dot{y}_2 - K_{sm}y_2 & y_2 \le 0 \end{cases} \quad (9)$$

$$F_{2R} = \begin{cases} 0 & y_2 < y_i \\ f_{sm}\dot{y}_2 + K_{sm}(y_2 - y_i) & y_2 \ge y_i \end{cases} \quad (10)$$

where

F_{2L} Seat reaction force for the left poppet of the second DCV, N
F_{2R} Seat reaction force for the right poppet of the second DCV, N

Flow rates through the throttling areas

There are two flow rates through the two throttling areas At_{21} and At_{23}(as shown in fig. 5). These flow rates are given by the following expressions:

$$Q_{21} = C_d At_{21} \sqrt{\frac{2(P_1 - P_2)}{\rho}} \quad (11)$$

$$Q_{23} = C_d At_{23} \sqrt{\frac{2(P_2 - P_t)}{\rho}} \quad (12)$$

where

Q_{21} Throttle flow rate of the left poppet of the second DCV, m^3/s
Q_{23} Throttle flow rate of the right poppet of the second DCV, m^3/s
At_{21} Throttle area of the left poppet of the second DCV, m^2
At_{23} Throttle area of the right poppet of the second DCV, m^2

Continuity equation of the valve chamber

There are two chambers (a) and (b) as shown in (fig. 5). The first chamber (a) is connecting the first and second valve together. The inlet flow rates of chamber (a) are Q_{11} and Q_{21}, while the output is Q_{13}. The continuity equation of the valve chamber (a) is:

$$Q_{11} - Q_{13} - Q_{21} = \frac{V_1}{B}\frac{dP_1}{dt} \quad (13)$$

where

V_1 Initial volume of chamber (a), 4 mm3
B Bulk modulus of oil, 1.9 GPa

Switching DCV Model

The switching DCV is displaced by the pressure forces, controlled by the direct operated DCV. The switching DCV is treated as (ON-OFF) switch for the main and secondary systems of the EHCS as shown in (fig. 6).

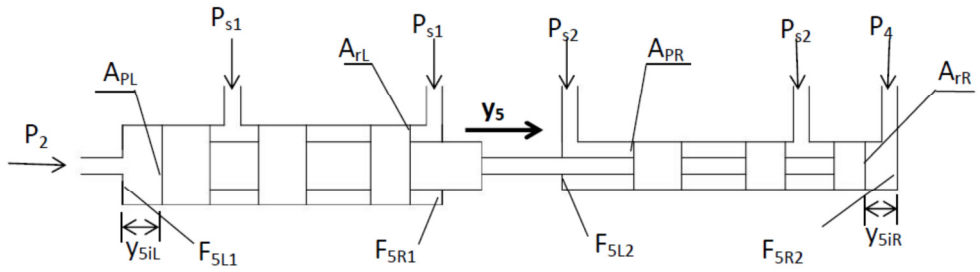

Fig. 6. Sliding DCV scheme.

Equation of motion

Its motion is described by this relation:

$$P_2A_{pL} - P_{s1}A_{rL} + P_{s2}A_{rR} - P_4A_{pR} - F_{SR5} = m_5\ddot{y_5} + f_5\dot{y_5} \quad (14)$$

where

A_{PL}	Left piston area, m^2
A_{rL}	Left rod side area, m^2
P_4	Pressure in the right chamber of the switching DCV, Pa
A_{rR}	Right rod side area, m^2
A_{PR}	Right piston area, m^2
y_5	Switching DCV displacement, m
m_5	Switching DCV mass, 0.05 kg
f_5	Switching DCV damping coefficient, $300\ Ns/m$
F_{sR5}	Total seat reaction force of the Switching DCV, N

Seat reaction force

There are four seat reaction forces effect on the SDCV (F_{5L1} , F_{5R1} , F_{5L2} and F_{5R2}). Their position is shown in (fig. 9).

$$F_{SR5} = F_{5R1} + F_{5R2} - F_{5L1} - F_{5L2} \quad (15)$$

$$F_{5R1} = F_{5R2} = \begin{cases} f_{sm}\dot{y_5} + K_{sm}(y_5 - y_{5iR}) & y_5 \geq y_{5iR} \\ 0 & y_5 < y_{5iR} \end{cases} \quad (16)$$

$$F_{5L1} = F_{5L2} = \begin{cases} -f_{sm}\dot{y_5} - K_{sm}(y_5 - y_{5iL}) & y_5 \leq y_{5iL} \\ 0 & y_5 > y_{5iL} \end{cases} \quad (17)$$

where

F_{5R1}	First right seat reaction force, N
F_{5R2}	Second right seat reaction force, N
F_{5L1}	First left seat reaction force, N
F_{5L2}	Second left seat reaction force, N
y_{5iR}	Right initial position of the switching DCV, 0.006 m
y_{5iL}	Left initial position of the switching DCV, 0 m

Continuity equation of the switching DCV chambers

The switching DCV has two chambers in the right and left sides. The left chamber is connected to the second DCV that has exit pressure P_2, but the right chamber is connected to the fourth DCV that has exit pressure P_4. Neglecting the internal leakage and the external leakage, the continuity equations of the valve chambers will be:

$$Q_{21} - Q_{23} - A_{PL}\dot{y_5} = \frac{V_2 + A_{PL}y_5}{B}\frac{dP_2}{dt} \quad (18)$$

$$Q_{41} - Q_{43} + A_{PR}\dot{y_5} = \frac{V_4 - A_{PR}y_5}{B}\frac{dP_4}{dt} \quad (19)$$

where

Q_{41}	Throttle flow rate of the left poppet of the fourth DCV, m^3/s.
Q_{43}	Throttle flow rate of the right poppet of the fourth DCV, m^3/s.

V_2 Initial volume of left chamber of the switching DCV, 6 mm^3.
V_4 Initial volume of right chamber of the switching DCV, 5 mm^3.

Two Stage EHSV Model

The EHCS contains two EHSV's; main and secondary EHSV. The dynamic behavior of main spool valve controlled by the main and secondary EHSV is described mathematically (neglecting the jet reaction forces), (fig. 7).

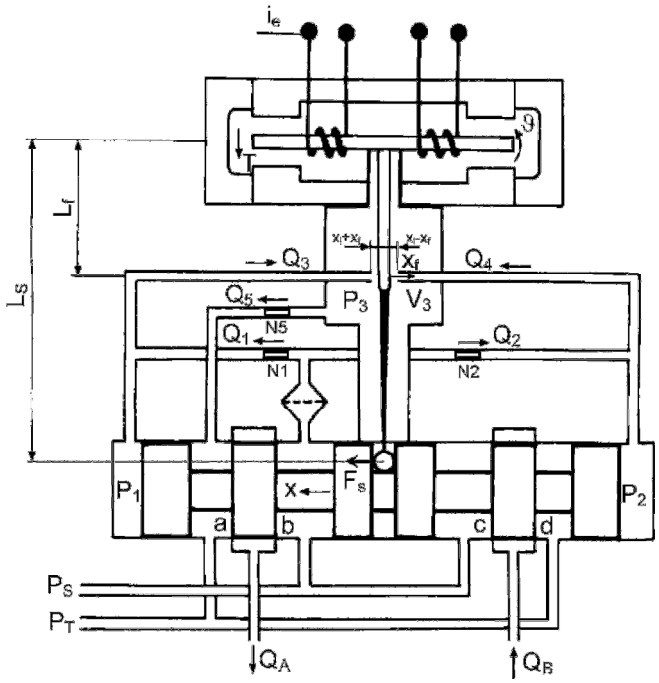

Fig. 7. EHSV scheme, [5].

Electromagnetic torque motor

The electromagnetic torque motor converts an electric input signal of low-level current (usually within 10 mA) into a proportional mechanical torque. The motor is usually designed to be separately mountable, testable, interchangeable, and hermetically sealed against the hydraulic fluid. The net torque depends on the effective input current and the flapper rotational angle. Neglecting the effect of the magnetic hysteresis, the following expression for the torque can be deduced:

$$T = K_i i_e + K_\theta \theta \tag{20}$$

where

T Torque of the electro-magnetic torque motor, Nm
i_e Torque motor input current, A
θ Armature rotation angle, rad
K_θ Armature rotational angle torque gain, 9.45*10^{-4} Nm/rad
K_i Current-torque gain, 0.556 Nm/A

Equation of motion of the armature

The motion of the rotating armature and attached elements is governed by the following equations:

$$T = J\ddot{\theta} + f_\theta\dot{\theta} + K_T\theta + T_L + T_P + T_F \quad (21)$$

$$T_P = \frac{\pi}{4} d_f^2 (P_{2L} - P_{1L}) L_f \quad (22)$$

where

J	Moment of inertia of the rotating part, $5*10^{-7}$ Nms^2
f_θ	Damping coefficient, 0.002 Nms/rad
K_T	Stiffness of flexure tube, Nm/rad
T_L	Torque due to flapper displacement limiter, Nm
T_P	Torque due to the pressure forces, Nm
T_F	Feedback torque, N.m
d_f	Flapper nozzle diameter, 0.5 mm
L_f	Flapper length, 9 mm

Feedback torque

The feedback torque depends on the spool displacement and the flapper rotational angle as given by the following equations:

$$T_F = F_s L_s \quad (23)$$

$$F_s = K_s(L_s\theta + x) \quad (24)$$

$$T_F = K_s L_s (L_s\theta + x) \quad (25)$$

where

F_s	Force acting at the extremity of the feedback spring, N
K_s	Stiffness of the feedback spring, 900 N/m
L_s	Length of the feedback spring and flapper, 30 mm
x	Main driven spool valve displacement, m

Flapper position limiter

The flapper displacement is limited mechanically by the jet nozzles. When reaching any of the side nozzles, the seat reaction develops a counter torque, given by the following equation:

$$T_L = \begin{cases} 0 & |x_f| < x_i \\ R_s\dot{\theta} - (|x_f| - x_i)K_{Lf}L_f & |x_f| > x_i \end{cases} \quad (26)$$

where

R_s	Equivalent flapper seat damping coefficient, 5000 Nms/rad
K_{Lf}	Equivalent flapper seat stiffness, $5*10^6$ N/m
x_f	Initial volume of left chamber, 6 mm^3
x_i	Flapper limiting displacement, 30 μm

Restriction areas

The restriction areas in the switching DCV and in the flapper valve are given by the following relations:

$$A_o = \frac{\pi}{4} d_f^2 \quad (27)$$

$$A_3 = \pi d_f (x_i + x_f) \quad (28)$$

$$A_4 = \pi d_f (x_i - x_f) \quad (29)$$

$$A_5 = \frac{\pi}{4} d_5^2 \tag{30}$$

$$A_{th} = \omega * |y_5| \tag{31}$$

$$A_{Bp} = \omega * |d_i - y_5| \tag{32}$$

$$x_f = L_f \theta \tag{33}$$

where

ω	Width of the port, 2 mm
A	Throttle area of the flapper nozzles, m^2
A_{th}	Throttle area of the EHSV entrance, m^2
A_{Bp}	By-pass area of the EHSV, m^2

Flow rates through switching DCV and flapper valve restrictions

The flow rates through the switching DCV and the flapper valve restrictions are given by the following equations:

$$Q_1 = C_d A_0 \sqrt{\frac{2(P_s - P_1)}{\rho}} \tag{34}$$

$$Q_2 = C_d A_0 \sqrt{\frac{2(P_s - P_2)}{\rho}} \tag{35}$$

$$Q_3 = C_d A_3 \sqrt{\frac{2(P_1 - P_3)}{\rho}} \tag{36}$$

$$Q_4 = C_d A_4 \sqrt{\frac{2(P_2 - P_3)}{\rho}} \tag{37}$$

$$Q_5 = C_d A_5 \sqrt{\frac{2(P_3 - P_t)}{\rho}} \tag{38}$$

$$Q_{th} = C_d A_{th} \sqrt{\frac{2(P_{s1} - P_s)}{\rho}} \tag{39}$$

$$Q_{Bp} = C_d A_{Bp} \sqrt{\frac{2(P_2 - P_1)}{\rho}} \tag{40}$$

where

Q	Flow rate of the flapper orifices areas, m^3/s
Q_{th}	Flow rate of the EHSV entrance, m^3/s
Q_{Bp}	By-pass flow rate of the EHSV, m^3/s
P_{sL}	Supply pressure to the EHSV, pa
P_1	Pressure in the left side of the flapper valve, Pa
P_2	Pressure in the right side of the flapper valve, Pa
P_3	Pressure in the flapper valve return chamber, Pa

Continuity equations applied to flapper valve chambers

Applying the continuity equation to the flapper valve chambers, neglecting the internal leakage and the external leakage, the following equations were obtained:

$$Q_1 + Q_{Bp} - Q_3 + A_s\dot{x} = \frac{V_0 - A_s x}{B}\frac{dP_1}{dt} \quad (41)$$

$$Q_2 - Q_{Bp} - Q_4 - A_s\dot{x} = \frac{V_0 + A_s x}{B}\frac{dP_2}{dt} \quad (42)$$

$$Q_3 + Q_4 - Q_5 = \frac{V_3}{B}\frac{dP_3}{dt} \quad (43)$$

$$Q_{th} - Q_1 - Q_2 = \frac{V_L}{B}\frac{dP_{sL}}{dt} \quad (44)$$

where

A_s	Spool cross-sectional area, m^2
V_0	Initial volume of oil in the spool side chamber, 2 cm^3
V_3	Volume of the flapper valve return chamber, 5 cm^3
V_L	Volume of left chamber in the switching DCV, 4 cm^3

Equation of motion of the spool

The motion of the spool valve is produced from the difference in pressure forces which act against seat reaction forces, viscous friction forces and inertia forces in the main and secondary EHSV's. The mathematical model of the main EHSV is deduced above in detail. For the secondary EHSV, its mathematical model is deduced by the same manner. The equation of motion of the main driven spool valve is described by:

$$(P_2 - P_1)A_s + (P_2 - P_1)A_s = m_s\ddot{x} + f_s\dot{x} + K_s L_s\theta + K_s L_s\theta + 2K_s\, x \quad (45)$$

where

m_s	Main spool valve mass, 0.1 kg
f_s	Spool friction coefficient, 50 Ns/m
P_2	Pressure in the left chamber of the EHSV, pa
P_1	Pressure in the right chamber of the EHSV, pa

SIMULATION RESULTS

The simulation results are obtained by the solver of ode23s (stiff/Mod. Rosenbrock). This solver is a variable step solver, which computes the model's state at the next time step using a modified Rosenbrock formula of order 2. The ode23s solver is a one-step solver, and therefore only needs the solution at the preceding time point. It is more efficient than ode15s at crude tolerances, and can solve stiff problems for which ode15s is ineffective.

Equations from (1) through (19) describe the behavior of the switching DCV. These equations are used to develop a computer simulation program using MATLAB/SIMULINK package. The result is plotted versus the time for t=0.1 second (fig. 8).

Equations from (1) through (45) describe the behavior of the whole EHCS. The transient response of the spool driven valve of the EHCS is obtained from the detailed model to a 10 mA step input current using the simulation program (as shown in fig. 9).

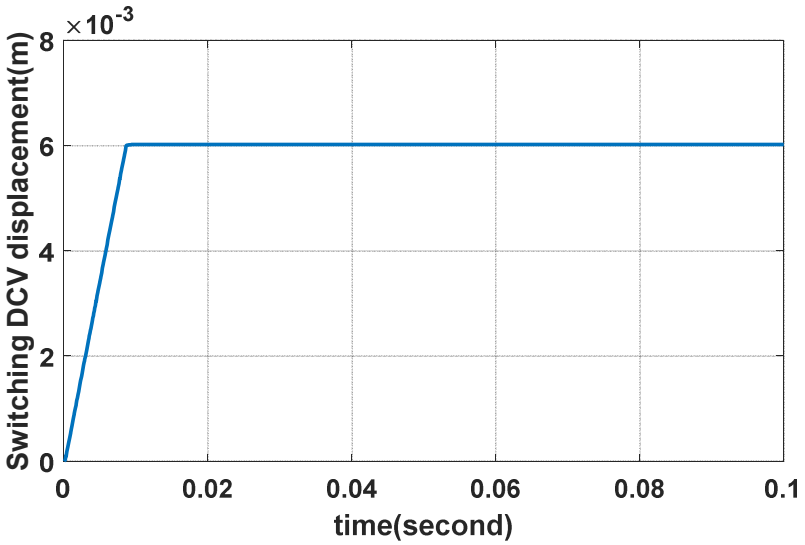

Fig. 8. Switching DCV displacement, y_5.

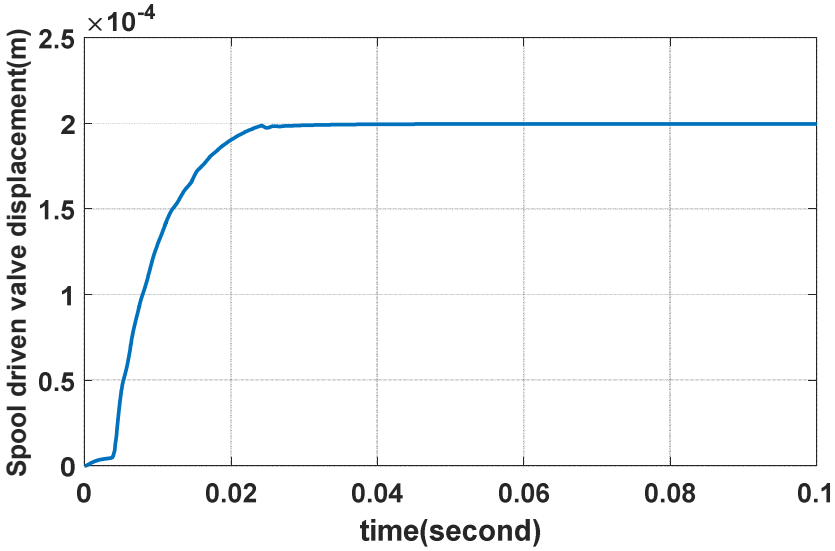

Fig. 9. Step response of the spool driven valve, x**.**

FAILURE MODES ANALYSIS

The failure modes are appearing mainly in the pressure sources or in the electrical input current signal to the solenoids and the servo-valves or a combination of them. In this case, the operation of the EHCS is called Emergency Operation. Some possible modes of failure; the failure of main pressure source, the main EHSV failure, and the combination of them, are presented in this work. Table 1 illustrates the discussed modes of failure.

In case of pressure source failure or de-energizing the solenoids in the main system, the communication of pressure from the secondary system to the right chamber of the switching DCV displaces it to the left. The EHSV of the main system is by-passed and the secondary system is put in charge to compensate for the failure in the main system operation.

Table 1. Modes of operation.

OPERATION DESCREPTION		EHSV		PRESSURE SUPPLY	
		Main SV	Secondary SV	Main P_{s1}	Secondary P_{s2}
Normal operation		1	1	1	1
Emergency operation	Main SV failure	0	1	1	1
	Main pressure source failure	1	1	0	1
	Main SV and Main pressure source failures	0	1	0	1

Figure (10a, 10b, and 10c) show the dynamic behavior of the EHCS to 10 mA step input current for each modes of failure. The steady state and the settling time values of the EHCS response are calculated and collected in Table 2.

Table 2. Response parameters.

OPERATION DESCRIPTION		STEADY STATE VALUE (mm)	SETTLING TIME (ms)
Normal Operation		0.1996	19.762
Emergency operation	Main SV failure	0.2039	19.699
	Main pressure source failure	0.2033	19.339
	Main SV and Main pressure source failures	0.2038	19.529

The EHCS response in the discussed modes of failure is approximately the same for the spool valve displacement with a steady state value of (~ $0.2\ mm$) and settling time of (~ $19.5\ ms$) with very small acceptable error in the these parameters as shown in fig. 10.

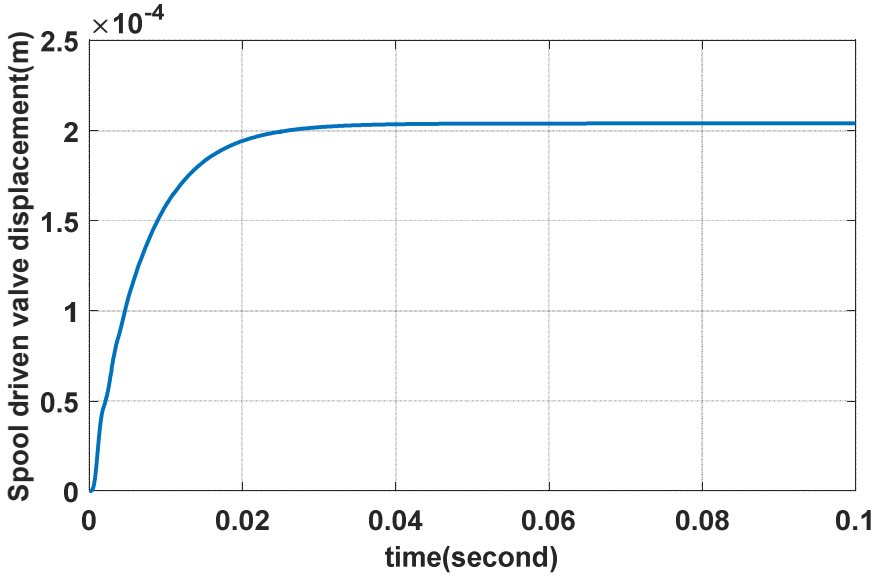

(a) Main EHSV failure**.**

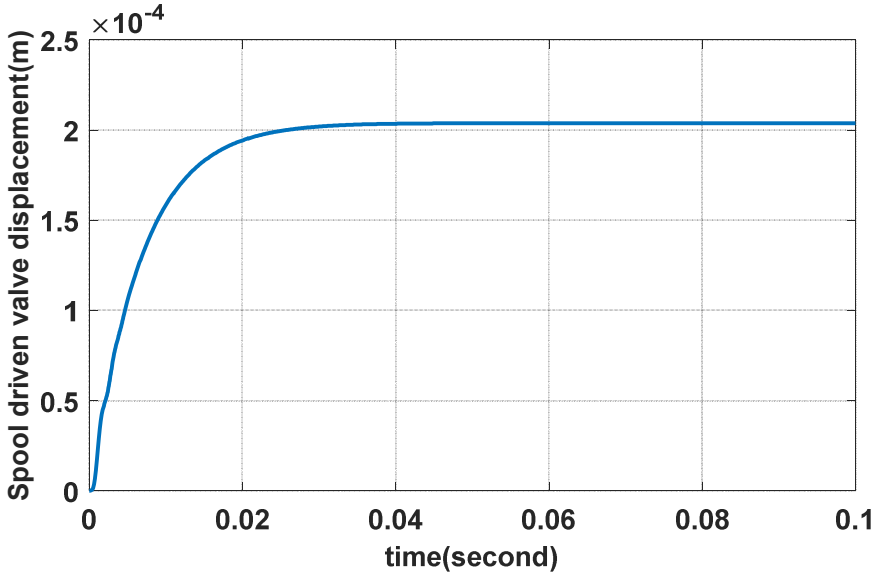

(b) Main pressure source failure.

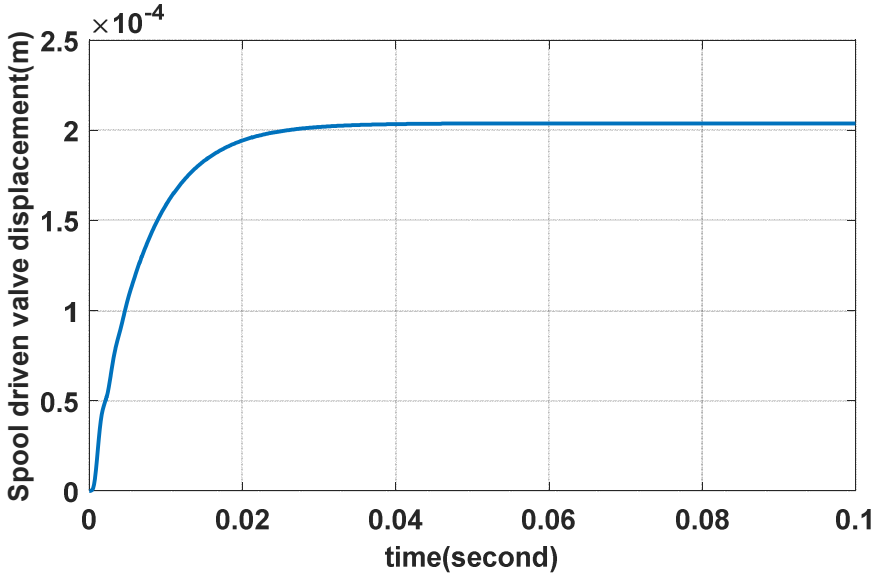

(c) Main EHSV and pressure source failures.

Fig. 10. EHCS step response in different modes of failure**.**

CONCLUSION

The safety of passengers and crew of a flying vehicle depends upon continued correct operation of the electro-hydraulic control system. The major work of this paper contains three aspects. First, the structure and working principle of the EHCS is analyzed. Second, a non-linear mathematical model and a computer simulation program are developed for the complicated EHCS. Third, the discussion of different failure modes; main EHSV, main pressure source failure, and a combination of them are presented. The simulation results showed that the EHCS presented has an acceptable transient response and the required output such that the main driven spool valve displacement is insured. This study show that this system is capable of

providing continued safe flight, even when experiencing certain component failure or combination of failures.

In future work, this system is a part of an integrated electro-hydraulic servo actuator (ISA) of a flying vehicle. These systems are used to position the maneuvering surfaces of the flying vehicles. So, the spool valve displacement obtained from this paper will be the essential input parameter to the hydraulic actuator module. This module will be presented to insure the maximum force, displacement, and the speed of the hydraulic cylinder. The system stability and precision will be insured by the implementation of convenient controllers.

REFERENCES

[1] M. A. A.-S. M. Galal Rabie, Mohammed Metwally, Tamer Nabil, Aerospace Applications of Fluid power, 2008.
[2] B. Chen and M. Lin, "The present research and prospects of electro-hydraulic servo valve", Chinese Hydraulics & Pneumatics, vol. 33, pp. 5-8, 2005.
[3] J. Cheng, et al., "Modeling and simulation for the electro-hydraulic servo system based on Simulink", in Consumer Electronics, Communications and Networks (CECNet), 2011 International Conference on, 2011, pp. 466-469.
[4] Y. Li, "Dynamic System Modeling and Simulation with Simulink (The second edition)", Xi'an University of Electronic Science and Technology Press, 2009.
[5] M. G. Rabie, "Fluid power engineering", vol. 28: McGraw-Hill New York, NY, USA, 2009.
[6] Z.-S. Wu, "Hydraulic control system", Beijing: Higher Education Press2008, 2008.
[7] Y.-J. Yang, et al., "Reliability analysis of electrohydraulic servo valve suffering common cause failures", Eksploatacja i Niezawodność, vol. 16, 2014.
[8] N. Mondal, et al., "A study on electro hydraulic servovalve controlled by a two spool valve", International Journal of Emerging Technology and Advanced Engineering, vol. 23, pp. 479-484, 2013.